



HAL
open science

Identification and characterization of thousands of bacteriophage satellites across bacteria

Jorge Moura de Sousa, Alfred Fillol-Salom, José Penadés, Eduardo P.C. Rocha

► **To cite this version:**

Jorge Moura de Sousa, Alfred Fillol-Salom, José Penadés, Eduardo P.C. Rocha. Identification and characterization of thousands of bacteriophage satellites across bacteria. 2022. hal-03838678v1

HAL Id: hal-03838678

<https://hal.science/hal-03838678v1>

Preprint submitted on 3 Nov 2022 (v1), last revised 21 Mar 2023 (v2)

HAL is a multi-disciplinary open access archive for the deposit and dissemination of scientific research documents, whether they are published or not. The documents may come from teaching and research institutions in France or abroad, or from public or private research centers.

L'archive ouverte pluridisciplinaire **HAL**, est destinée au dépôt et à la diffusion de documents scientifiques de niveau recherche, publiés ou non, émanant des établissements d'enseignement et de recherche français ou étrangers, des laboratoires publics ou privés.



Distributed under a Creative Commons Attribution - NonCommercial - NoDerivatives 4.0 International License

1 Identification and characterization of thousands of bacteriophage 2 satellites across bacteria

3 Jorge A. Moura de Sousa^{1,*}, Alfred Fillol-Salom², José R. Penadés² and Eduardo P.C. Rocha^{1,*}

4
5 ¹Institut Pasteur, Université Paris Cité, CNRS, UMR3525, Microbial Evolutionary Genomics,
6 Paris 75015, France ²MRC Centre for Molecular Bacteriology and Infection, Imperial College
7 London, London, SW7 2AZ, UK

8 * corresponding authors: jorge-andre.sousa@pasteur.fr, erocha@pasteur.fr

9 Abstract

10 Bacteriophage-bacteria interactions are affected by phage satellites, elements that exploit
11 phages for transfer between bacterial cells. Satellites can encode defense systems, antibiotic
12 resistance genes, and virulence factors, but their number and diversity are unknown for lack
13 of a tool to identify them. We developed a flexible and updateable program to identify satellites
14 in bacterial genomes – SatelliteFinder – and use it to identify the best described families: P4-
15 like, phage inducible chromosomal islands (PICl), capsid-forming PICl, and phage-inducible
16 chromosomal island-like elements (PLE). We vastly expanded the number of described
17 elements to ~5000, finding hundreds of bacterial genomes with two different families of
18 satellites, and dozens of *Escherichia coli* genomes with three. Most satellites were found in
19 Proteobacteria and Firmicutes, but some are in novel taxa such as Actinobacteria. We
20 characterized the gene repertoires of satellites, which are variable in size and composition,
21 and their genomic organization, which is very conserved. With the partial exception of PICl
22 and cfPICl, there are few homologous core genes between families of satellites, and even
23 fewer homologous to phages. Hence, phage satellites are ancient, diverse, and probably
24 evolved multiple times independently. Occasionally, core genes of a given family of satellites
25 are found in another, suggesting gene flow between different satellites. Given the many
26 elements found in spite of our conservative approach, the many bacteria infected by phages
27 that still lack known satellites, and the recent proposals for novel families, we speculate that
28 we are at the beginning of the discovery of massive numbers and types of satellites.
29 SatelliteFinder is accessible for the community as a Galaxy service at
30 [https://galaxy.pasteur.fr/root?tool_id=toolshed.pasteur.fr/repos/fmareuil/satellitefinder/Satellit](https://galaxy.pasteur.fr/root?tool_id=toolshed.pasteur.fr/repos/fmareuil/satellitefinder/SatelliteFinder/0.9)
31 [eFinder/0.9](https://galaxy.pasteur.fr/root?tool_id=toolshed.pasteur.fr/repos/fmareuil/satellitefinder/SatelliteFinder/0.9)

32 Keywords: Mobile Genetic Elements, Phage Satellites, Horizontal Gene Transfer,
33 Comparative Genomics.

34 Introduction

35

36 Bacteriophages (phages) shape the evolution and composition of bacterial communities, both
37 through predation and by driving horizontal gene transfer between bacterial cells (1, 2).
38 Phages are notorious parasites of bacteria and are themselves parasitized by phage satellites.
39 These elements lack some of the functions required for autonomous horizontal transfer, which
40 they hijack from helper phages. In the past, phage satellites were sometimes mistaken for
41 defective phages, even if their gene repertoires rarely have genes in common with phages.
42 Yet, some phage satellites do have phage-like genes. For example, the phage-inducible
43 chromosomal islands (PICI) of *Staphylococcus aureus* typically encode packaging functions
44 homologous to those of the helper phage 80 α (3, 4). In contrast, the P4 satellite of *Escherichia*
45 *coli* has few homologs with its P2 helper phage (5). Phage satellites exploit their helper phages
46 through molecular mechanisms that depend on the type of satellite. The extent of this
47 exploitation is variable, as are its consequences for phage reproduction. Phage-inducible
48 chromosomal island-like elements (PLE) of *Vibrio cholerae* completely block the propagation
49 of the helper lytic phage ICP1 (6) and PICI can severely reduce phage reproduction (7). On
50 the other hand, the recently identified capsid-forming PICI (cfPICI) EcCIEDL933 of *E. coli* has
51 negligible effects on phage fitness (8). Beyond their effect on phage infection, satellites provide
52 their bacterial hosts with accessory potentially adaptive functions. For example, some PICI
53 encode virulence factors, like toxins, or antibiotic resistance genes (3), and some P4-like
54 elements and PICI encode anti-phage immunity systems (9, 10). Hence, satellites have wide
55 functional and ecological impacts in phages and in bacteria.

56

57 The few satellites that have been studied in detail encode a set of core functions that are
58 sometimes non-homologous but can be grouped into four major groups: integration,
59 regulation, replication and hijacking. All known satellites are integrated in chromosomes,
60 which usually occurs by the action of an integrase of the Tyrosine recombinase family. Upon
61 excision, satellites require specific replicases to replicate before being packaged in viral
62 particles. Genetic regulation is essential for the success of the element. On one hand, the
63 element may remain for long periods of time largely silent in the chromosome before entering
64 in contact with an infecting helper phage. On the other hand, upon co-infection by a helper
65 phage, the satellite must coordinate its expression with the latter. One of the most fascinating
66 traits of satellites is the diversity of mechanisms they use to subvert the host phage viral
67 particles. Some phage satellites physically constrain the size of the viral capsid produced by
68 the phage, so that phage DNA does not fit inside – but the satellite DNA does (11). Other

69 satellites directly redirect the packaging of their own DNA into the viral capsid by encoding
70 sequences that mimic the phages' terminases (12).

71

72 Phage satellites have only recently emerged as a distinct class of mobile elements. Even if
73 the satellite P4 was discovered decades ago, few phage satellites have been detected in
74 genomes until very recently. Also, some of these mobile elements were either mistaken as
75 plasmids (13) or annotated as defective phages or prophage-like remains (14). However, this
76 perspective has recently changed. There is increasing evidence of the pervasiveness and
77 importance of phage satellites (15, 16), and recent work has started to uncover the diversity
78 of these elements, especially within a given family (5, 12). These studies have helped
79 recognize phage satellites as characteristic mobile elements that have specialized in being
80 mobilized by fully functional phages. Moreover, there have been recent reports of genomic
81 islands transduced by phages that are different from known phage satellites, which suggests
82 that different types of satellites remain to be discovered (17, 18).

83

84 Many studies have unraveled the mechanisms of function of the model satellites for each of
85 the known families, as well as their importance in bacterial evolution and pathogenicity (4, 9,
86 10, 19). But their abundance in genomes is poorly studied for lack of a systematic way to
87 identify them. This is important, because the small number of known phage satellites has
88 limited their comprehensive study in terms of evolution and diversity. Recently, we have
89 reported the discovery of ca 1000 elements of the P4-like family, which has led to novel
90 insights regarding their diversity, evolution, genomic composition and organization (5). Here,
91 we systematize and expand this analysis to all currently known phage satellite families and
92 report the discovery of more than 5000 putative phage satellites in complete bacterial
93 genomes. This allowed us to study the abundance of phage satellites within and across
94 bacterial hosts, and to understand how the different families of satellites are organized in terms
95 of their core components and genetic repertoires. We also sought to understand whether there
96 are similarities between the different main families of phage satellites, and whether there are
97 different sub-families within them. Our approach allows for a novel, automatic detection of
98 phage satellites, of all known families, in bacterial genomes and sheds light on the abundance
99 and diversity of these mobile elements.

100

101 Methods

102 Genomic datasets

103

104 We retrieved all the complete genomes of the NCBI non-redundant RefSeq database
105 (<ftp://ftp.ncbi.nlm.nih.gov/genomes/refseq/>, last accessed in March 2021), including 21086
106 bacteria, 21520 plasmids and 3725 phages. We also retrieved and syntactically annotated
107 both complete and draft genomes of *Vibrio* spp (n=11627 in total), using PanACoTA (version
108 1.3.1 (20)), ran with the Singularity module. We used the methods “prepare -s <species>”
109 (where <species> was iteratively replaced with the most representative species of
110 Vibrionacea: *Vibrio*, *Aliivibrio*, *Enterovibrio*, *Photobacterium*, *Grimontia*, *Salinivibrio* and
111 *Thaumasiovibrio*, databases accessed in March 2022), with the options “--min 0 --max 0.4”,
112 for the MASH distance thresholds (21). We then used the method “predict --prodigal” to
113 syntactically annotate the genomes.

114

115 Overall strategy for detection of phage satellites

116

117 There are only a few experimentally verified satellites. This means that we cannot use machine
118 learning methods to identify the elements at this stage. Instead, we made a curated annotation
119 of a large set of known satellite elements and used them to iteratively identify core genes of
120 each family of satellites. We then designed individual and customizable MacSyFinder (22, 23)
121 models that represent the genetic composition of the different phage satellite families (**Fig S1**).
122 The models were used in MacSyFinder to identify occurrences of the putative satellites.
123 MacSyFinder missed a few elements in certain genomic contexts or was unable to disentangle
124 tandem occurrences of similar satellites. Hence, to improve the methods, we developed a
125 post-processing script, which also provides a classification of the satellite variants (**Fig S2**).

126

127 Throughout the process of optimizing the detection of satellites, we sometimes identified
128 components that are less conserved than expected and were thus removed from the list of
129 core genes. Also, some genes were found to be more conserved than expected and were
130 included as core components. As a result, we iterate the entire process again, until very few
131 changes occur between iterations. At each iteration we verify that most of the known satellites
132 are accurately classified. In the following sections, we describe the key steps of the process
133 that leads to our method of detecting phage satellites. The details associated with each family
134 of satellites are given in the initial paragraphs of each section of the results, and the tables
135 with all the satellites identified are given in **File S1**.

136

137 [Modelling of satellite-like systems](#)

138

139 We made an iterative enrichment and curation of the core (marker) components based on the
140 analysis of genomic regions in bacterial genomes that could correspond to putative satellites.

141

142 1) We collected genomic regions containing the pre-defined components at less than a pre-
143 defined distance, to minimize the detection of components of tandem elements. For example,
144 two components are clustered if they are less than 10 genes apart. We make a transitive
145 clustering of the components, i.e., when one advances linearly in the genome sequence the
146 cluster is closed and evaluated only when meeting a succession of more than 10 genes lacking
147 a marker. If the cluster contains enough marker genes, i.e. it meets the minimal quorum, it is
148 kept for further analysis. We checked at this stage that the procedure identified the known or
149 previously proposed satellites and does not match known phages.

150

151 2) We took these clusters and built their pangenome to identify the most abundant gene
152 families in each phage satellite family. The pangenomes were built by clustering all the
153 candidate proteins at a minimum of 40% identity, using mmseqs2 (24) (version 13-45111),
154 with parameters `-cluster_mode 1` and `-min_seq_id 0.4` (all other parameters were left as
155 default). The clusters of abundant gene families are usually good markers for the presence of
156 a satellite.

157

158 3) The resulting gene families were functionally annotated using PFAM (release 33.1) and
159 bactNOG (25).

160

161 4) Sometimes a family that was not initially used as a marker was found to be present at high
162 frequency in #2. In such cases, we checked if an adequate HMM profile was available in
163 PFAM. If this was not the case the HMM profile was built as described above. In any case, the
164 inclusion of novel profiles implicated re-starting the process (back to #1).

165

166 5) We tested if we should define groups of marker genes as “exchangeable”. In such cases,
167 MacSyFinder will fill the quorum of a marker if it identifies one of a set of protein profiles. For
168 example, integrases of the Tyrosine recombinase and of the Serine recombinase families are
169 often found as functional analogs in mobile genetic elements. To identify these exchangeable
170 elements, we used the literature (for analogs) or searched the known satellites for analogous
171 components. Introduction of “exchangeable” components led us back to #1.

172

173 6) We varied the parameter of maximal distance between consecutive components to test how
174 it affects the method. When the analysis revealed that we should extend this distance because
175 some frequent gene families were often found a bit further downstream, we adapted this
176 parameter. If this increased the frequency of a gene family up to the point where it could be
177 used as a marker, we started again at #1. In the cases presented in this study, a distance of
178 10 or 15 genes was regarded as a good trade-off between identifying a few unusually long
179 elements and preventing the frequent aggregation of several satellites into one cluster.

180

181 7) Sometimes we added components in the models to improve the discrimination between
182 different families of satellites, or between satellites and prophages. In most cases, this was
183 done by including some “forbidden” components that are almost never found in one family of
184 satellites. For example, tail proteins are never (or very rarely) found in satellites and allow to
185 distinguish them from prophages. When such markers were added, we started again at #1.

186

187 This iterative procedure resulted in a MacSyFinder model for each family of satellites. These
188 models were used to systematically search for putative phage satellites in bacterial genomes.
189 The MacSyFinder models for each satellite family are available within the Docker package of
190 SatelliteFinder (https://hub.docker.com/r/gempasteur/satellite_finder).

191

192 Identification of markers and construction of HMM profiles

193

194 The first step in identifying novel satellites is to characterize the known ones and identify the
195 genes that are most frequently associated with them (markers). We collected the satellites
196 experimentally verified or proposed as homologs in previous publications and clustered them
197 by 40% (or 20%, for cases where no clusters emerged) protein sequence similarity. This
198 revealed families of proteins that were the most frequent in a given family of satellite. The
199 majority of these frequent components was adequately identified by existing HMM profiles of
200 the PFAM database. When this was not the case, we built custom HMM profiles by aligning
201 all sequences of the family with Clustal Omega (26) (Version 1.2.3) with default parameters,
202 and then by using hmmbuild (default parameters) from hmmer 3.3.2 (27).

203

204 Identification of putative phage-satellites with MacSyFinder

205

206 We used MacSyFinder (22, 23) (version 2.05rc) to provide a reproducible, shareable, and
207 easily modifiable tool to identify phage satellites in bacterial genomes. Briefly, MacSyFinder
208 searches for co-occurrence of the markers of each phage satellite family in bacterial genomes.
209 The criteria for the identification of the occurrences of markers and for the acceptable patterns
210 of co-occurrence can be defined by the user and that is what we call a model. MacSyFinder
211 reports the cases with highest scores, namely where the largest co-occurrence of the different
212 markers was found. For example, a genomic region with all markers gets a higher score than
213 a genomic region with fewer markers.

214

215 Typically, one searches for these markers either using curated thresholds or by providing an
216 e-value cutoff. Here, we lacked previous information on protein sequence diversity in the
217 satellites and we tried to maximize the sensitivity of the models relative to this parameter.
218 Hence, we used general and relaxed cutoffs (e-value < 0.01 and coverage > 40%, with
219 parameters “--no-cut-ga --i-evalue-sel 0.01 --coverage-profile 0.4” in MacSyFinder), to detect
220 distant homologs. The MacSyFinder model requires the identification of a number of markers
221 and their co-occurrence. The need to respect a minimum quorum of co-localized components
222 decreases the rate of false positives that could arise from the use of relaxed criteria of
223 sequence similarity, because false positive satellites would require the random simultaneous
224 co-localization of individual false positive markers. A specific concern arises with degraded
225 prophages that could resemble some satellites. These are discussed in the corresponding
226 results section. The remaining parameters of MacSyFinder were left as default.

227

228 [Post-processing of MacSyFinder results](#)

229

230 The use of MacSyFinder alone allows to find most of the known or previously proposed
231 satellites (**Table S1**). Yet, we noticed that a few elements were lost in some families (e.g.,
232 10% of cfPIC1 elements). This is caused by two features of the program that we corrected by
233 post-processing the results.

234

235 1) Clusters of genes with a match to at least one forbidden profile are rejected. This
236 feature is required to distinguish satellites with markers often found in phages from
237 phages themselves, or to distinguish between different satellite families with many
238 homologous core components. However, sometimes satellites and prophages are
239 contiguous in bacterial genomes and the forbidden component is on the flanking
240 element, not on the satellite itself. Hence, we post-process the results to include those
241 discarded due to the presence of one single “forbidden” component in the cluster (to

242 allow for unknown variants) and those where the “forbidden” component is outside of
243 the cluster of components (prophages contiguous to satellites). These “rescued”
244 clusters are very rare for most satellite types (see Results section). They are
245 specifically identified in the output of our scripts and in our analyses in the main text.

246

247 2) MacSyFinder outputs the largest possible cluster of markers of satellites, which may
248 result in merging multiple satellites. It may also merge satellites with small contiguous
249 mobile elements having an integrase. Our post-processing starts by handling the
250 occurrence of multiple integrases and then focuses on tandem satellites. First, we
251 search for the presence of multiple integrases (we assume there should be only one).
252 If so, we choose the one that is closest to the other (non-integrase) components, and
253 use any other integrase as a starting point of a new set of components. This procedure
254 may thus output several putative satellites from a single MacSyFinder cluster.

255

256 The MacSyFinder output lists the markers present in each putative satellite. For the analysis
257 of the number and types of components present in the latter, we post-process the output to
258 classify putative satellites into “types”: (A) have all (N) core components, (B) have N-1 core
259 component, (C) have N-2 core components, and so on. These types are further categorized
260 as “variants” that correspond to the component(s) that are missing. We note that many Type
261 B and C elements are complete and functional, since some correspond to elements that were
262 experimentally verified and many are very conserved. They may correspond to a variant of
263 the prototypical satellite that either completely lacks a given marker component (e.g., due to
264 gene loss or pseudogenization), has a non-homologous analog of the component, or has a
265 diverged component that was not detected.

266

267 [Genomic comparison of phage satellites with weighted gene-repertoire](#) 268 [relatedness \(wGRR\)](#)

269

270 We searched for sequence similarity between all proteins of phages and/or satellites using
271 mmseqs2 (24) with the sensitivity parameter set at 7.5. The results were converted to the blast
272 format and we kept for analysis the hits respecting the following thresholds: e-value lower than
273 0.0001, at least 35% identity, and a coverage of at least 50% of the proteins. The hits were
274 used to retrieve the bi-directional best hits between pair of genomes, which were used to
275 compute a score of gene repertoire relatedness weighted by sequence identity (28):

276
$$wGRR = \frac{\sum_i^p id(A_i, B_i)}{\min(A, B)}$$

277

278 where A_i and B_i is the pair i of homologous proteins present in A and B , $id(A_i, B_i)$ is the
279 sequence identity of their alignment, and $\min(A, B)$ is the number of proteins of the genome
280 encoding the fewest proteins (A or B). $wGRR$ is the fraction of bi-directional best hits between
281 two genomes weighted by the sequence identity of the homologs. It varies between zero (no
282 bi-directional best hits) and one (all genes of the smallest genome have an identical homolog
283 in the largest genome). $wGRR$ integrates information on the frequency of homologs and
284 sequence identity. For example, when the smallest genome has 10 proteins, a $wGRR$ of 0.2
285 can result from two homologs that are strictly identical or five that have 40% identity. The
286 hierarchical clustering of the $wGRR$ matrix, and the corresponding heatmap, were computed
287 with the *clustermap* function from the *seaborn* package (version 0.11.1, developed for Python
288 3.9), using the Ward clustering algorithm.

289

290 Calculation of diversity of bacterial hosts

291

292 We assessed the diversity of the phage satellites' bacterial hosts using two measures. The
293 Species Diversity (S) is the number of bacterial species where at least one phage satellite was
294 identified. Since the genome datasets are very unbalanced, with some species accounting for
295 a large fraction of genomes, the Species Diversity measure can misrepresent the true diversity
296 of the hosts of satellites. Hence, we use also Shannon's diversity index (H') (29) for each
297 phage satellite family. The index is calculated according to the formula:

298
$$H' = - \sum_{i=1}^R p_i \ln(p_i)$$

299 Where R is the total number of bacterial species with at least one satellite, and p_i is the
300 proportion of satellites found in the i th bacterial host species, in relation to the total number of
301 satellites for the corresponding family (e.g., if there is a total of 500 elements, and 300 are
302 found in *E. coli* genomes, $p_{E.coli}=0.6$). Thus, a family of satellites where the vast majority of
303 elements is located in only a few bacterial species will have a lower Shannon diversity index
304 than a family of satellites that is equally spread across bacterial species.

305 Phylogenetic analysis

306

307 We aggregated in single fasta files all the protein sequences corresponding to either the
308 regulatory, capsid or small terminase components of both PICI and cfPICI genomes. The
309 sequences were aligned using mafft-linsi (30) (v. 7.490, default parameters) and the resulting
310 alignment trimmed with clipkit (31) (v. 1.3.0, default parameters). We then used IQ-Tree (32)
311 (v. 1.6.12) to build the phylogenetic trees, with the options `-bb 1000` to run the ultrafast
312 bootstrap option with 1000 replicates and `-nt 6`. The resulting tree files were visualized and
313 edited using the v5 webserver of iTOL (33).

314

315 [Availability](#)

316

317 We provide the MacSyFinder models and the customized python scripts to perform the
318 abovementioned post-processing as a tool we call SatelliteFinder, that is available as a Docker
319 package (https://hub.docker.com/r/gempasteur/satellite_finder) and also a Galaxy server
320 interface (34)
321 (https://galaxy.pasteur.fr/root?tool_id=toolshed.pasteur.fr/repos/fmareuil/satellitefinder/SatelliteFinder/0.9).

323

324 Results

325 P4-like satellites are frequently found in Enterobacterial genomes

326

327 The P4 satellite is among the best studied satellites (11, 35, 36). P4 hijacks P2 capsids through
328 physical constraining, in order to encapsidate its own DNA. Our previous work has shown that
329 the P4-like family of satellites contains seven very conserved components (5). We used this
330 information to build MacSyFinder models to detect P4-like satellites (see Methods). We
331 searched for the co-occurrence of an integrase with six other components: Psu, Delta and Sid,
332 which are involved in the hijacking of the capsid of the P2 helper phage; a regulatory protein,
333 typically homologous to AlpA (although we also search for homologs of MerR or Stl as other
334 possible regulators); Ash (also called ϵ), which inactivates the repressor of the helper phage,
335 causing its induction; and α , a protein with primase and helicase activities that is required for
336 P4 replication.

337

338 The P4 MacSyFinder model identified a similar amount (1054 vs 1037) of P4-like elements
339 relative to our previous search in the same database (5). Around 90% of the elements were
340 in the same bacterial host genome and started at the same integrase gene. We used this
341 model to search for P4-like elements in a much larger dataset of 21086 bacterial genomes
342 (**Fig 1**). We more than doubled the number of putative P4-like satellites previously identified
343 (2160). The majority (1621) of these elements encode all the seven core components
344 (henceforth called Type A, **Fig 1A and 1B**), whilst 350 elements lacked one of them (Type B).
345 The missing component may be absent, be non-identifiable by the protein profile, or may be
346 replaced by a functional analog (see Methods). The most abundant of these variants lacks
347 Psu (Type B#var06). Since Sid and Psu are structural homologs (37) it is possible that some
348 variants of the former may compensate for the absence of the latter. There are 189 elements
349 that lack two core components (Type C), most often ϵ and α (Type C#var01) or AlpA and α
350 (Type C#var02). The vast majority of putative P4-like phage satellites (93%) were detected in
351 Enterobacteriaceae, where 35% of the bacterial genomes encode from one to three of these
352 elements (**Fig 1C and 1D**). Other bacterial families with P4-like elements include Yersiniaceae
353 (23% of the genomes with at least one element), where variants lacking Psu are prevalent,
354 Pectobacteriaceae, Erwinaceae and Hafniaceae. All but one P4-like elements are integrated
355 in bacterial chromosomes, confirming that these elements are usually not present in cells as
356 plasmids.

357

358 Consistent with our previous analysis, the organization of the core components of P4-like
359 satellites is conserved. Type A and the most frequent Type B variants encode the *psu-delta-*
360 *sid* operon, followed by *alpA*, ϵ and α (**Fig 1E** and **Fig S3A**), with each component usually
361 found in the same relative location (**Fig S3B**). We delimited the element between the integrase
362 and its farthest core component, discarding those lacking an integrase. The resulting 2097
363 P4-like elements have a median size of 10Kb and a median of 11 genes (**Fig 1F**, **Fig 1G**). A
364 small minority of these (<2%) is larger (between 15 and 22Kb).

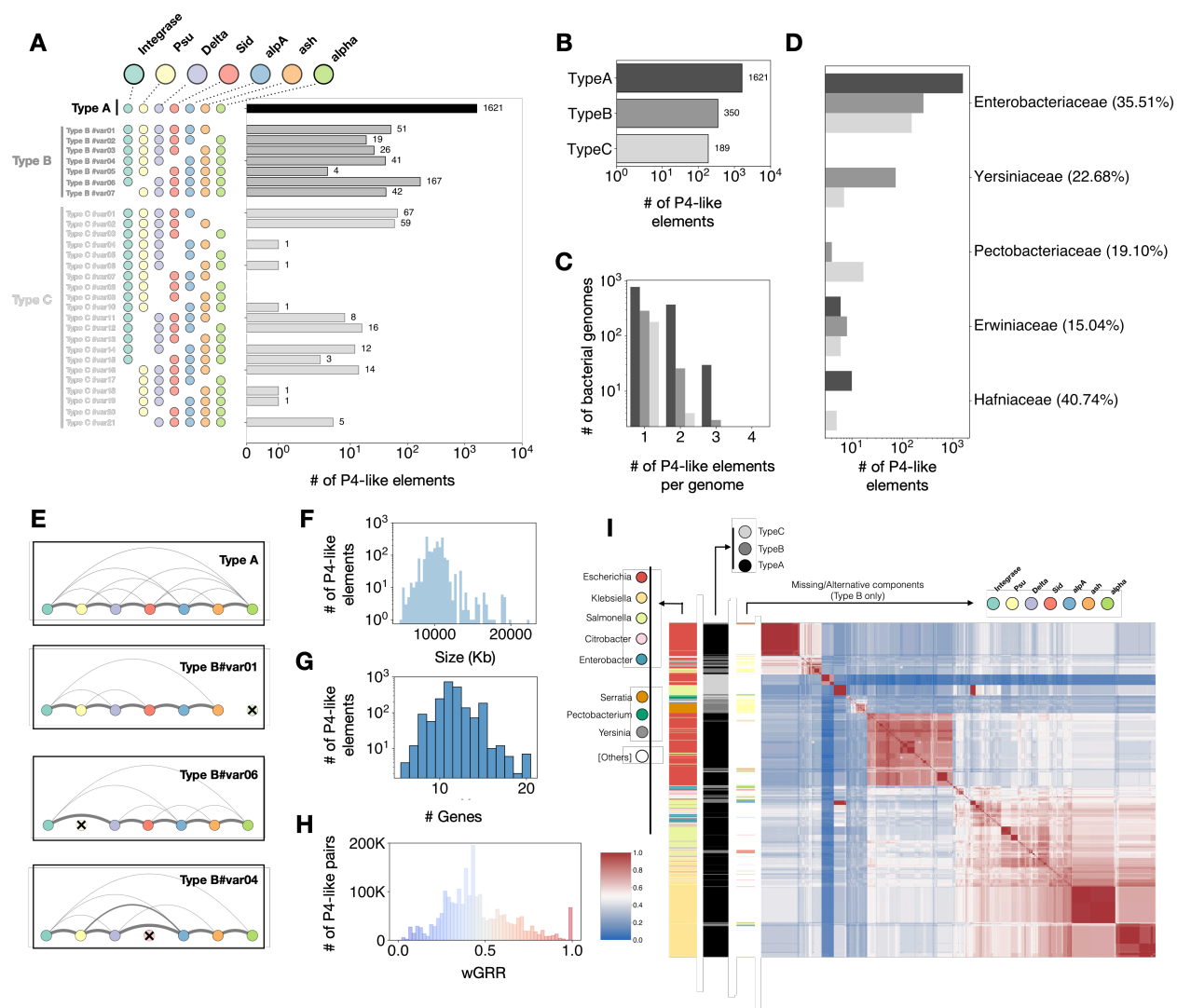
365

366 We measured the similarity between P4-like elements using weighted gene repertoire
367 relatedness (wGRR, see Methods). Some elements are identical (peak at wGRR=1 in **Fig 1H**),
368 but most of them are only moderately related. The median wGRR is 0.42. We clustered them
369 in relation to wGRR to assess their similarities (**Fig 1F**). There are two distinct sub-families
370 within *Escherichia* genomes, and an additional large family including mainly elements found
371 in *Salmonella* and *Klebsiella* genomes, but also in *Enterobacter* and *Citrobacter*. Other
372 subfamilies include other clades such as *Serratia*, *Yersinia* and *Salmonella*. The subgroup of
373 elements specific to *Salmonella* are all of Type C, as are the small family of elements in
374 *Escherichia* genomes that form a very distinctive subfamily at the top of the matrix in **Fig 1F**.
375 Many elements lack the same core genes and are associated with specific clades. This
376 suggests that these are not defective elements. Instead, they seem to form distinctive variants
377 (or subfamilies) of the P4 family. If the functions of the missing core genes in these variants
378 are facultative, or if they can be complemented by other components remains unknown.

379

380 Although subfamilies tend to be associated with specific bacterial hosts, we also found some
381 very similar elements in different species. This suggests of horizontal transfer of P4-like
382 satellites across distant bacteria. We found 3182 pairs of very similar elements in different
383 bacterial species (4% of those with wGRR \geq 0.9). Some very similar (wGRR > 0.8) pairs can
384 also be found in different families (280 pairs, e.g., between Enterobacteriaceae and Hafniaceae,
385 or Erwiniaceae). Together, these results reinforce our previous findings of a large (and now
386 even larger) family of P4-like phage satellites with a characteristic and conserved genomic
387 organization and a broad host range.

388



389
390
391
392
393
394
395
396
397
398
399
400
401
402
403
404

Figure 1. The abundance, genetic organization, bacterial hosts and genomic structure of the family of P4-like elements. **A)** Number of the different variants of P4-like elements identified in bacterial genomes. **B)** Total number of the different types of P4-like elements. **C)** Total number of P4-like genomes per bacterial genome. **D)** Distribution of P4-like elements in bacterial families. The percentages in front of each family correspond to the proportion of genomes of that family where (at least) one P4-like element was inferred. **E)** Genomic organization of the four most frequent variants of P4-like satellites. Nodes correspond to the different markers of the satellite (variants where the marker is absent have that indicated as a crossed-out node) and the edges between the nodes represent the frequency with which those two components are contiguous (but not necessarily adjacent). **F)** Distribution of the sizes of the extracted genomes of P4-like elements. **G)** Distribution of the number of proteins contained within each P4-like genome, for the elements detected in the two different bacteria datasets. **H)** Distribution of the pairwise wGRR values between all the P4-like genomes. **I)** Symmetric heatmap of the matrix of the wGRR values ordered using hierarchical clustering. The colours follow the same code as in **(H)** with blue pixels representing low wGRR values (dissimilar genomes) and red pixels representing high wGRR values (similar genomes). The columns to the left of the heatmap indicate the bacterial species where the P4-like genome was detected, the Type (A, B or C) of the P4-like genome, and the component that is missing for given variants (exclusively for elements of Type B).

405 Phage Inducible Chromosomal Islands (PICI) are diverse and widespread across 406 bacterial phyla

407
408 PICI include the *Staphylococcus aureus* pathogenicity islands (SaPI) that were extensively
409 studied, as well as numerous other elements present in both diderm and monoderm bacteria
410 (12, 38). The described PICI have a conserved genetic organization and five core components
411 found in almost all known elements: (i) integrase, (ii) regulation module (homolog to *alpA*,
412 *merR* or *stfI*), (iii) primase-replicase module, (iv) capsid morphogenesis (more frequent in PICI
413 from Proteobacteria), encoding a protein that is thought to modify the morphology of the
414 hijacked capsids to block the encapsidation of phage DNA, (v) small terminase subunit,
415 responsible for redirecting the packaging of the capsid to the satellite's DNA. While other
416 accessory genes are normally encoded by PICI (notably between the integrase and the
417 regulation or the primase-replication module, or after the *terS* homolog), PICI typically do not
418 encode other phage-like structural or lysis genes. We used the core components to detect
419 PICI (**Fig S1B**). Given the homologs between PICI, cfPICI and prophages, we included in the
420 PICI model several "forbidden" components to discriminate them accurately from the others
421 (see Methods): tail, holin, and cfPICI components described below.

422
423 Our approach identified 1436 putative PICI, the vast majority (>99.9%) in chromosomes (**Fig**
424 **2A and B**): 375 (26%) with the five core components (Type A), and 1061 (74%) with four
425 (Type B). We note that a small number of them (31, 2%) were initially rejected by MacSyFinder
426 due to the presence of one forbidden gene near (but outside) the cluster of PICI-like core
427 components. They were recovered by post-processing the results (see Methods). The vast
428 majority (97%) of the elements with all core components (Type A) are found in *Escherichia*
429 *coli* genomes. The other variants are found across much more diverse bacterial hosts (**Fig**
430 **2D**), including in 66% of Mycobacterial genomes (including *M. tuberculosis*) and 35% of
431 Staphylococcaceae genomes. Some of the latter were previously identified as SaPIs. They
432 are known to lack the capsid morphogenesis gene typically found in Enterobacterial PICI
433 because they rely in a different hijacking strategy (3). Thus, these variants are *bona fide*
434 functional PICI, experimentally observed to be mobilized by helper phages. We also detected
435 more than 6000 elements with three core genes (Type C). These may be functional satellites,
436 but the small number of core genes increases the probability that they may be defective PICI,
437 other mobile genetic elements, or just random aggregates of PICI-like functions (for instance,
438 a typical P4-like satellite is classified as a Type C PICI because it encodes an integrase, AlpA
439 and a primase/replicase). Hence, in order to remain conservative in our analysis, we focused
440 on PICI-like elements of Type A and B.

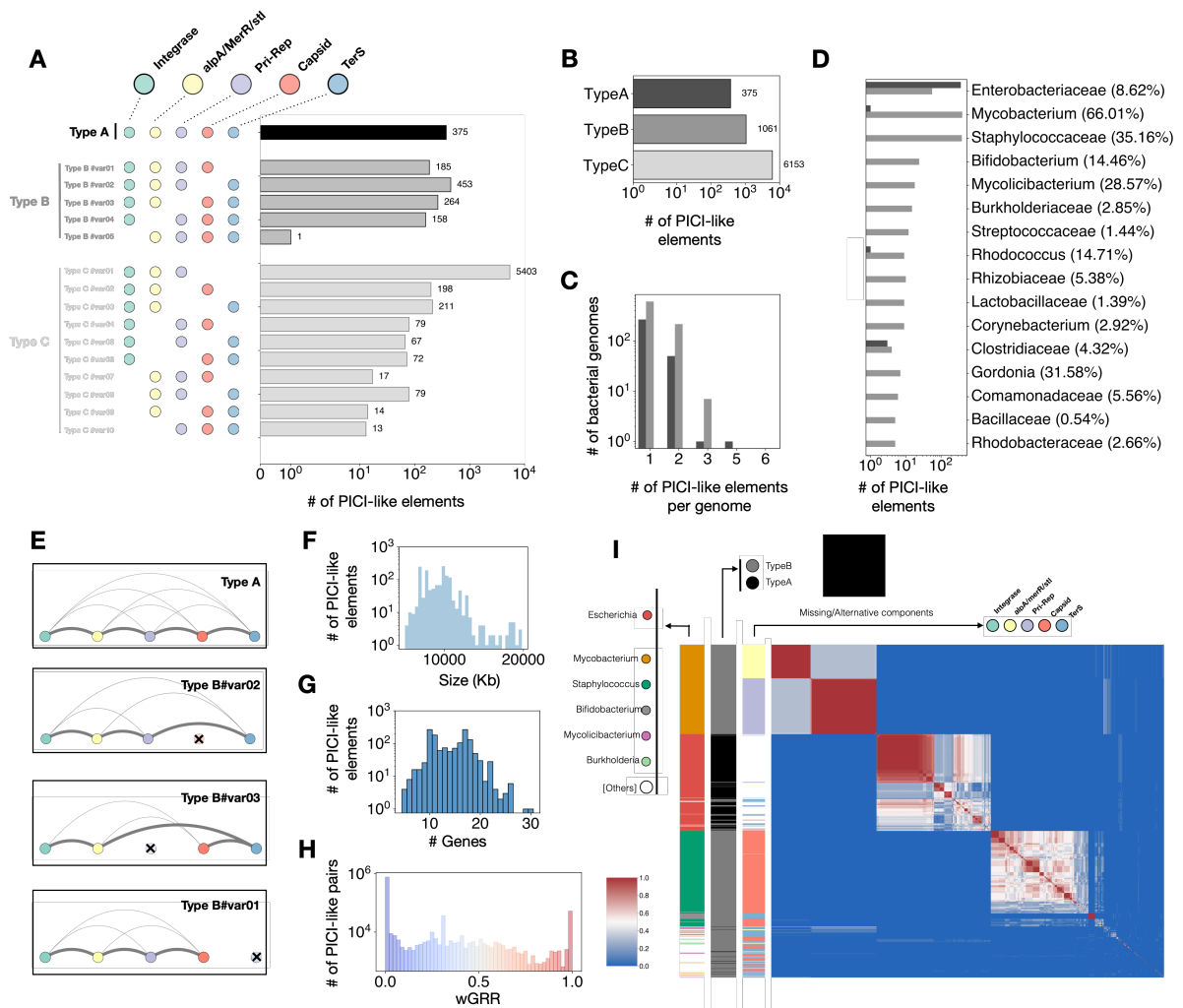
441
442
443
444
445
446
447
448
449
450
451
452
453
454
455
456
457
458
459
460
461
462
463
464
465
466
467
468
469
470
471
472
473
474
475
476

PIC1 are present in many more species (190) than P4-like elements (81). These hosts are very diverse, including bacteria where phage satellites were not previously known to exist, and that are important in clinical and/or ecological settings. For instance, we detected putative PIC1 in *Acinetobacter*, *Bacillus* (as well as *Lactobacillus*), *Burkholderia*, *Clostridium*, *Rhodococcus* or *Sinorizhobium*. However, as most elements are found in a few (over-sequenced) bacterial genus (e.g., *Escherichia*, *Mycobacterium* and *Staphylococcus*), the difference in diversity considering the overrepresentation of PIC1 in certain bacterial taxa is less marked (Shannon Index = 2.55 for hosts of PIC1 elements versus 2.14 for hosts of P4-like elements). Some bacterial genomes can have up to five PIC1, even if most bacteria have one or two of these elements (**Fig 2C**).

The organization of the PIC1 core components is well conserved, as suggested by previous studies and mentioned above (12) (**Fig 2E** and **Fig S4**). Only one of the most common variants shows a different order (Type B#var03, with a missing/unidentified primase-replicase), where the small terminase gene tends to be found before the capsid. We used the region from the integrase to the last identified core component to delimit the PIC1 (the element lacking the integrase was discarded). The resulting 1435 PIC1 have a median size of 9.5Kb (15 proteins), and only a few elements (17) have between 20 and 28Kb (**Fig 2F**, **Fig 2G**).

PIC1 are much more diverse, as measured by the wGRR, than P4-like satellites ($p=0$, two-sample Kolmogorov-Smirnov test). Their set of core components is smaller and most pairs of PIC1 have a very low wGRR (**Fig 2H**). The wGRR matrix groups PIC1 in four very distinct sub-families, each predominantly associated with a bacterial clade: *Escherichia* (two sub-families), *Mycobacterium*, and *Staphylococcus* (**Fig 2I**). Most elements in Mycobacteria tend to be very similar, forming two clusters with either an unidentified regulator or a primase-replicase. All the genomes of the putative satellites in *M. tuberculosis* (which are the majority of putative phage satellites identified in this taxon) are very similar to the previously described “small prophage-like elements” PhiRv1 and PhiRv2 (39, 40). Yet, other putative Mycobacterial phage-satellites are genetically distinct from the latter, and found across different species (e.g., in *M. abscessus*) (**Fig S5**). The *Staphylococcus* PIC1 lack a capsid modification gene, as previously described (12), and are split in many smaller subgroups. Those of *Escherichia* are very divergent and form smaller subgroups. There are also many small clusters of PIC1s that each represent those few elements found in the genomes of other bacteria, and most of these PIC1 have four identified core components.

477 There are relatively few obvious cases of putative intra-species transfer of PICI. Only 73 pairs
 478 of elements with a high wGRR are found in different bacterial species (0.1% of the total number
 479 of pairs with wGRR > 0.9, n=60107). A large fraction is found in two *Staphylococcus* spp.,
 480 although we do find some rare cases of putative transfer between more distant bacteria (e.g.,
 481 *Acetivibrio* and *Tissierellia*). Thus, relative to P4-like satellites, PICI seem to be less frequently
 482 transferred across phylogenetically distant bacterial hosts. This may be a consequence of the
 483 presence of a majority of these elements in three very distantly related bacterial genera.
 484 Overall, these results uncover a plethora of very diverse PICI that are present in a large range
 485 of bacterial hosts.
 486
 487



488
 489 **Fig. 3. The abundance, genetic organization, bacterial hosts and genomic structure of the PICI family.** A)
 490 Number of the different variants of PICI-like elements identified in bacterial genomes. B) Total number of the different types of
 491 PICIs. C) Total number of PICIs per bacterial genome. D) Distribution of PICIs of Type A or B in bacterial families. The
 492 percentages in front of each family correspond to the proportion of genomes of that family where (at least) one PICI was inferred.
 493 E) Genomic organization of the four most frequent variants of PICIs. Nodes correspond to the different markers of the satellite
 494 (variants where the marker is absent have that indicated as a crossed-out node) and the edges between the nodes represent the

495 frequency with which those two components are contiguous (but not necessarily adjacent). **F)** Distribution of the sizes of the
496 extracted genomes of PICIs. **G)** Distribution of the number of proteins contained within each PICIs, for the elements detected in
497 the two different bacteria datasets. **H)** Distribution of the pairwise wGRR values between all the genomes of PICIs. **I)** Symmetric
498 heatmap of the matrix of the wGRR values ordered using hierarchical clustering. The colours follow the same code as in **(H)** with
499 blue pixels representing low wGRR values (dissimilar genomes) and red pixels representing high wGRR values (similar
500 genomes). The columns to the left of the heatmap indicate the bacterial species where the PICI genome was detected, the Type
501 (A or B) of the PICI, and the component that is missing for given variants (exclusively for elements of Type B). The putative
502 elements that were initially rejected by MacSyFinder, but that we included in the analysis, do not form a particular, segregated
503 subcluster (**Fig S6**), suggesting they might be *bona fide* PICI.
504

505 Capsid-forming Phage Inducible Chromosomal Islands (cfPICI) are a novel and 506 distinct type of PICI

507
508 The cfPICI are a novel family of satellites related with PICI, but with a unique trait: they
509 assemble their own cfPICI-specific capsid (8). Yet, cfPICI are incapable of forming viable
510 phage particles because they lack other structural genes that they hijack from the helper
511 phage, *e.g.* holins and tail-associated proteins. The presence of structural genes in cfPICI
512 makes them more difficult to discriminate from prophages. For this reason, we defined profiles
513 associated with phage tails, or phage holins, as forbidden components in the cfPICI model.

514
515 Five core components of cfPICI are homologous or analogous to the five core components of
516 PICI, and in some cases the leftmost part of cfPICI (comprising the integrase, regulator and
517 primase) were found to be exactly the same as PICI (8), suggesting they are indeed
518 evolutionarily related. Some others are occasionally also found in PICI. This is the case of a
519 nuclease (HNH) that is essential for phage head morphogenesis (and DNA packaging) in fully
520 functional phages (41) and a head decoration module (a serine protease). We postulate that
521 some of these genes might be used for the modification and stabilization of capsid morphology
522 for phage capsids hijacked by PICI. However, there are several specific core components of
523 cfPICI that allow to distinguish them from PICI: genes involved in the attachment of capsid to
524 the hijacked tails (head-tail adaptor and head-tail connector), and a gene encoding the large
525 terminase protein (*terL*) (**Fig S1C**).

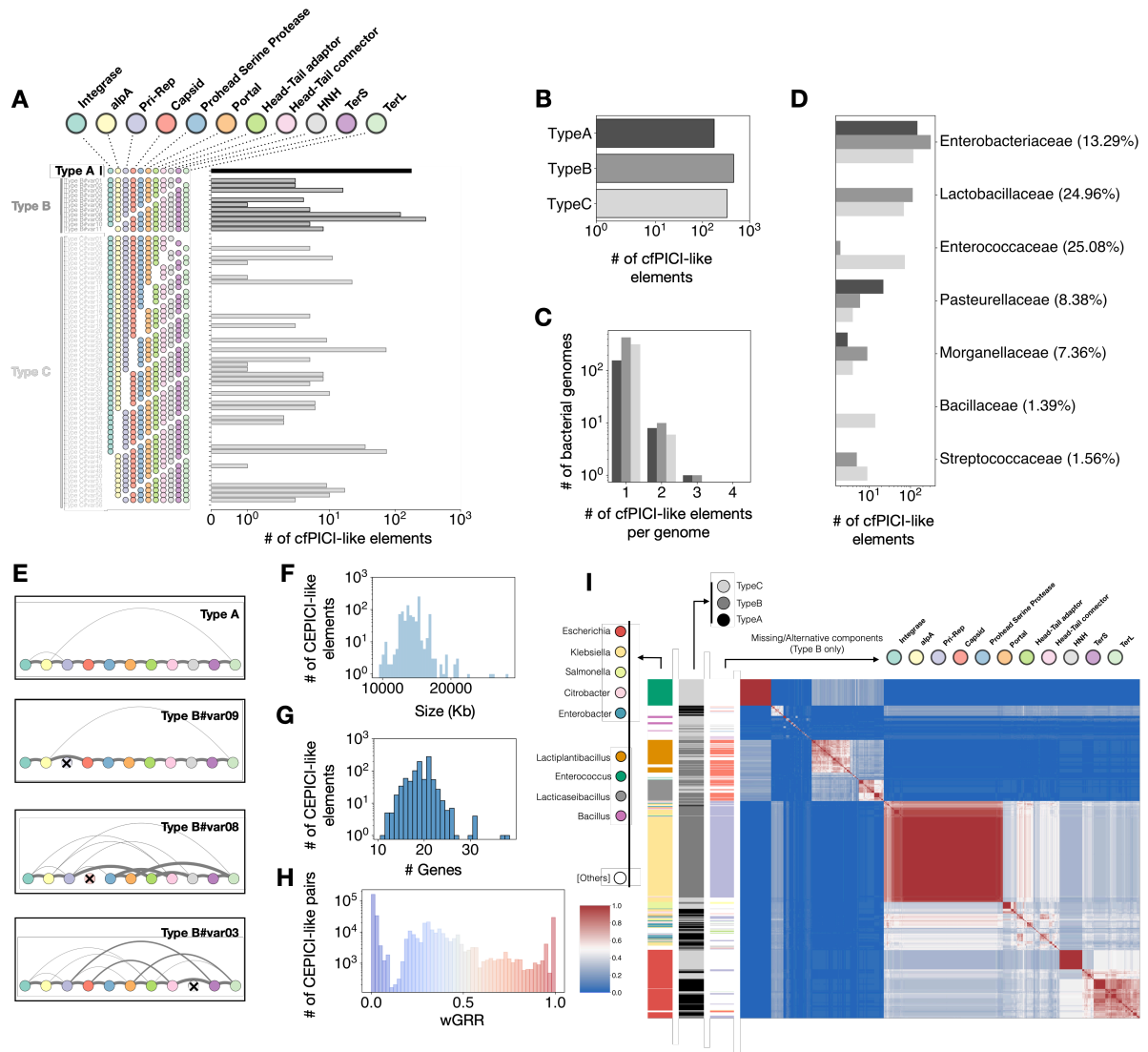
526
527 We detected 969 cfPICI, all but three in chromosomes. Among these cfPICI, 177 had all the
528 11 core components (Type A), 459 had 10 (Type B), and 333 had 9 (Type C) (**Fig 3A and**
529 **3B**). 73 of cfPICI (<8%) were initially rejected by MacSyFinder due to the presence of a nearby
530 gene homologous with either a single tail or holin gene. They were retrieved in the post-
531 processing step because the forbidden component is outside the cfPICI (see Methods). Type
532 A cfPICI were exclusively found in Proteobacteria. They are very abundant in

533 Enterobacteriaceae (13% of all genomes), and in Pasteurellaceae (8%) and Morganellaceae
534 (7%) (**Fig 3D**). Variants of cfPICI within Firmicutes tend to have the capsid component merged
535 with the prohead serine protease component (and therefore genes matching exclusively the
536 capsid can be absent). As MacSyFinder reports the best scoring profile for each gene, the
537 latter is chosen instead of the capsid profile(s). These cfPICI are frequently found in
538 Lactobacillaceae (25%) and Enterococcaceae (25%), and rarer (<2%) in Bacillaceae and
539 Streptococcaceae. Overall, cfPICI are found in more species than PICI or P4-like elements
540 (136, Shannon Index = 3.1), and are again present in several important species, where phage
541 satellites have not been detected (e.g., from the genus of *Bacillus*, *Bordetella*, *Citrobacter*,
542 *Haemophilus*, *Pseudomonas* or *Xanthomonas*).

543
544 The genomic organization of the core components of cfPICI is very conserved, with the
545 exception of two variants that are more diverse (**Fig 3E** and **Fig S7**). We extracted the
546 proteomes of the putative cfPICI, defined between the integrase and the farthest core
547 component, after discarding five unusually large elements (>30kb) and the 48 elements
548 without integrase. The remaining 916 putative cfPICI have a median size of 14Kb and encode
549 a median of 19 proteins.

550
551 The gene repertoires of cfPICI are more similar than those of PICI, with a median wGRR of
552 0.2 and almost 10% of pairs with a wGRR higher than 0.8. Clustering the cfPICI by their wGRR
553 reveals several subfamilies, usually associated with either monoderms (e.g., *Enterococcus*
554 and *Lactobacillus*) or Proteobacteria (mostly *Escherichia*, *Klebsiella*, *Salmonella* and
555 *Citrobacter*). This fits the previously obtained phylogeny of these elements (8). Within these
556 sub-families, cfPICI tend to be more similar between closely related hosts. The cfPICIs added
557 by the post-processing script (e.g., with neighboring prophage genes) integrate the existing
558 clusters, suggesting that they are valid elements (**Fig S8**). Although there is a strong
559 association between cfPICI subfamilies and particular bacterial hosts, c.a. 9% of the cfPICI
560 pairs with a high wGRR (>0.9, n=36173) were detected in different host species. For instance,
561 some cfPICI of *K. pneumoniae* are very similar to those found in *Salmonella*, *Enterobacter* or
562 *Citrobacter*. This suggests that, relative to PICI, cfPICI are potentially capable of disseminate
563 across more phylogenetically distant hosts.

564
565
566
567



568

569

570

571

572

573

574

575

576

577

578

579

580

581

582

583

584

Fig. 3. The abundance, genetic organization, bacterial hosts and genomic structure of the cfPICI family. A) Number of the different variants of cfPICIs identified in bacterial genomes. This includes elements that were initially rejected by MacSyFinder but recovered with our post-processing analysis, and correspond to 38, 15 and 20 of Types A, B and C, respectively) **B)** Total number of the different types of cfPICIs. **C)** Total number of cfPICIs per bacterial genome. **D)** Distribution of cfPICIs in bacterial families. The percentages in front of each family correspond to the proportion of genomes of that family where (at least) one cfPICI was inferred. **E)** Genomic organization of the four most frequent variants of cfPICIs. Nodes correspond to the different markers of the satellite (variants where the marker is absent have that indicated as a crossed-out node) and the edges between the nodes represent the frequency with which those two components are contiguous (but not necessarily adjacent). **F)** Distribution of the sizes of the extracted genomes of cfPICIs. **G)** Distribution of the number of proteins contained within each cfPICI genome. **H)** Distribution of the pairwise wGRR values between all the cfPICIs. **I)** Symmetric heatmap of the matrix of the wGRR values ordered using hierarchical clustering. The colours follow the same code as in (H) with blue pixels representing low wGRR values (dissimilar genomes) and red pixels representing high wGRR values (similar genomes). The columns to the left of the heatmap indicate the bacterial species where the cfPICI genome was detected, the Type (A, B or C) of the cfPICI, and the component that is missing for given variants (exclusively for elements of Type B).

585 Phage-inducible chromosomal island-like elements (PLEs) are mostly clonal and
586 are specific to *Vibrio cholerae*

587

588 PLEs were described in *Vibrio cholerae*, where they play a critical role in the defense from the
589 virulent phage ICP1 (6). So far, all described PLEs are specific to *V. cholerae* (19) even if
590 recently other putative satellites with homology to a few PLE genes were described in other
591 *Vibrio* species (e.g., *Vibrio parahaemolyticus*) (42). PLEs excise from the chromosome and
592 package their genomes by hijacking ICP1. The cost for ICP1 is exacerbated by the
593 acceleration of lysis promoted by PLEs after their packaging (43), which effectively halts the
594 spread of ICP1 in the population.

595

596 To determine the core components of PLEs, we first selected the homologs present in at least
597 three of the five prototypical PLE genomes (PLE 1 to 5 (6)). We treated differently the
598 components most distant from the integrase because they are more variable; hence, we
599 selected those found in at least two of the five prototypical PLEs. We used the core
600 components for the iterative search of putative PLEs in the Vibrionaceae genomes (see
601 Methods), which resulted in the selection of a large number (15) of highly frequent markers for
602 PLE. Some of these markers have a well-defined role in the PLE lifecycle: an integrase, a
603 gene that represses the capsid morphogenesis of ICP1 (*capR*), a replication initiation protein
604 (*repA*), a nickase that hampers the replication of the hijacked phage (*nixI*), and a gene that
605 accelerates the lysis of the bacterial host cell (*lidl*). Other highly frequent markers of PLE to
606 which we were able to assign a functional PFAM annotation include a protein with an HTH
607 binding domain, which was previously described in PLEs (6); a sigma 70-like factor, a
608 component of the specificity subunit of the bacterial RNA polymerase; and a profile with
609 homology to a cyclin-dependent kinase-activating kinase (MAT1) suggested to be involved in
610 nucleotide excision repair of damaged DNA (44). Seven other highly frequent markers (M1 to
611 M7) were uncharacterized, and we were unable to annotate them using PFAM. Given the
612 substantial variation in terms of presence/absence of these markers in the known PLE
613 genomes (see **Table S1**), we used all the 15 markers to study the natural variation of this
614 satellite family.

615

616 PLE are specific of a few *Vibrio* and are rare in our original dataset. To increase the sample
617 size, we retrieved from Genbank all complete and draft genomes of Vibrionacea (11627
618 genomes, see Methods). We detected 410 elements of Types A to I, i.e., with between all
619 (Type A) and 7 (Type I) PLE markers (**Fig 4A**). Most genomes have a single PLE. Some of
620 these types correspond to known variants of previously identified PLEs. Elements of Type A

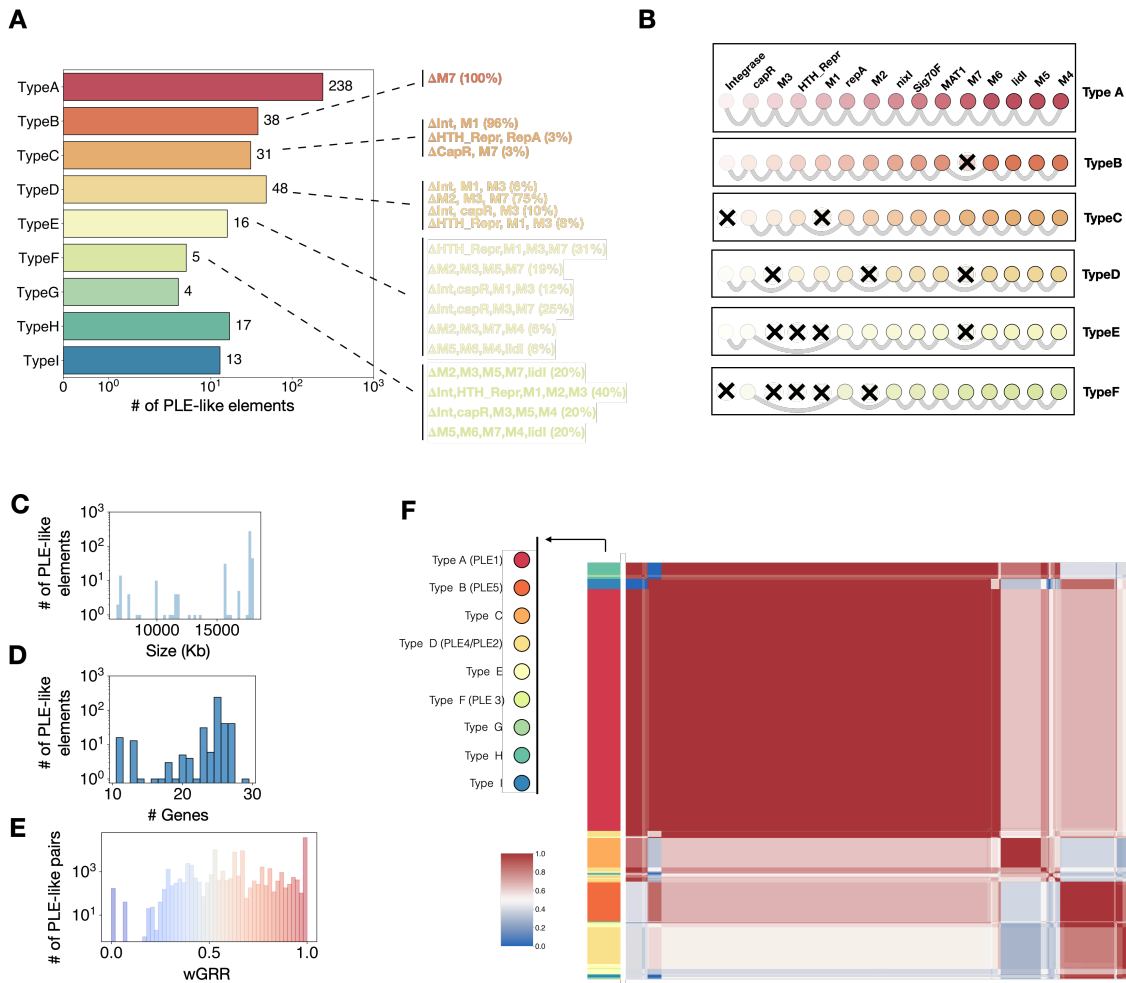
621 (n=238) correspond to PLE1 and elements of Type B (n=38), for which we only find a single
622 variant, correspond to PLE5. PLE2 and PLE4 correspond to two different variants of Type D
623 and PLE 3 corresponds to a variant of Type F (**Table S1**). The more incomplete elements
624 (Types G, H and I) tend to either lack or have highly distinct first or final half of the PLE markers
625 we assembled, and it is likely that they result from assembling artifacts inherent to draft
626 genomes. All the putative PLE-like satellites detected in the Vibrionaceae dataset were found
627 in *V. cholerae* (in 12% out of its 3446 total genomes for this species).

628

629 The core components present across the PLE variants are very diverse (**Fig 4B**), but the order
630 of the components is extremely well conserved (**Fig 4C**). We extracted the region between
631 the integrase and the furthest component (typically M4) in Type A elements. These regions
632 have a median size of 17.7Kb (and 25 proteins). These elements tend to be genetically very
633 similar, with more than 90% of the pairs having wGRR values higher than 0.9. Further, 12
634 genomes are enough to regroup all other satellites at $wGRR \geq 0.9$, i.e., the remaining genomes
635 are very similar to one of these (**Fig 4F**). While this may seem contradictory with the
636 observation that several core genes are often missing, PLE differ from the other elements in
637 that a large fraction of genes are core. Some of these 12 groups were much more abundant
638 than others, leading to a few very large clusters (**Fig 4F**). Overall, our results further confirm
639 that PLEs are very distinctive from other satellites and have limited genetic diversity, forming
640 highly related sub-families around the previously known PLE types.

641

642



643

644

645 **Fig. 4. The abundance, genetic organization, and genomic structure of PLEs.** **A)** Number of the different types of PLEs
 646 identified in Vibrionaceae genomes. Dashed lines in front of the bars indicate the variants within each type, more specifically
 647 which components are missing/undetected. The proportion of each variant is shown in parentheses. **B)** Genomic organization of
 648 the most frequent variant for each PLE type. Nodes correspond to the different markers of the satellite (variants where the marker
 649 is absent/unidentified have that indicated as a crossed-out node) and the edges between the nodes represent the frequency with
 650 which those two components are contiguous (but not necessarily adjacent). **C)** Distribution of the sizes of the extracted genomes
 651 of PLEs. Although we extracted genomes for all identified sets, we do not use those that are found between contigs (1.2%) to
 652 account for the distribution in genome size, as the precise genomic locations (and relative distances) of the proteins would be
 653 unreliable. **D)** Distribution of the number of proteins contained within each PLE genome. **E)** Distribution of the pairwise wGRR
 654 values between all the PLE genomes (in both bacterial datasets). **F)** Symmetric heatmap of the matrix of the wGRR values
 655 ordered using hierarchical clustering. The colours follow the same code as in (E) with blue pixels representing low wGRR values
 656 (dissimilar genomes) and red pixels representing high wGRR values (similar genomes). The column to the left of the heatmap
 657 indicate the type of PLE (in parenthesis, the prototypical PLEs that are classified with a similar type).

658

659

660 Phage-satellite families form genetically distinct groups of mobile elements and
661 can co-exist in bacterial genomes

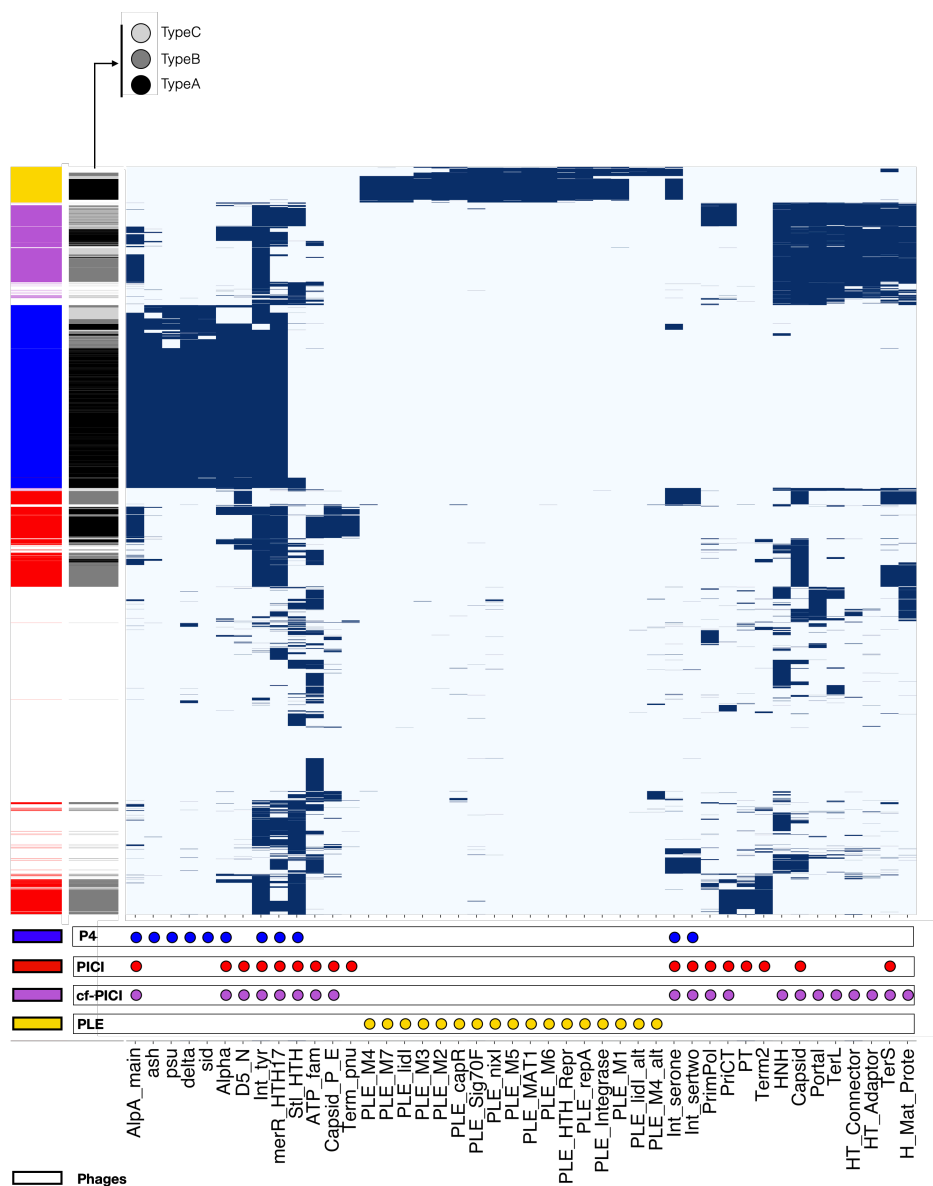
662

663 All satellites exploit functional phages for mobilization, but the mechanisms involved in this
664 process differ widely. This raises questions regarding the evolutionary origin of these
665 elements, in particular whether they diversified from a single ancient satellite, or if they evolved
666 multiple independent times. To understand the similarities between the different families of
667 satellites, we analysed the co-occurrence of core genes from all satellite families across all
668 the putative phage satellite genomes identified. For each satellite, we note the
669 presence/absence of each core gene. The resulting binary matrix with all satellites was
670 clustered (**Fig 5**) and revealed that three of the four families (P4-like, cfPICl and PLE), form
671 well-separated and cohesive clusters of elements. PICl aggregated in multiple clusters, which
672 is consistent with their high gene repertoire diversity (**Fig 2I**). Interestingly, the separation of
673 satellites in different clusters is due to the combination of their markers, and not due to the
674 presence or absence of a single one. For instance, AlpA is found in all P4-like, in many cfPICl
675 and in some PICl. Moreover, the same gene can match two regulatory profiles (e.g., *alpA* and
676 *merR*), although sometimes a single satellite genome can also have two regulatory genes,
677 each matching a different protein profile. This analysis also occasionally identified satellites of
678 a given family encoding components that are core from another. For instance, some cfPICl
679 have a homolog of ϵ from P4, some P4-like satellites have a homolog of HNH from cfPICl, and
680 some PLEs have a TerS homologous to that of PICl and cfPICl. These results show that the
681 different families of satellites are clearly distinct, but they also suggest gene flow of core genes
682 between satellite families.

683

684 Our analysis could mistakenly annotate phages as satellites, because they have homologous
685 components. To test this, we retrieved the genomes of 3725 phages and made an analysis
686 similar to that done with the satellites. Almost all phages have at least one homolog to a
687 satellite core gene. This is expected because both often have an integrase and capsid-
688 associated genes. Nevertheless, there are rarely more than a few of these core genes in
689 common between phages and satellites. The clustering of the large binary matrix of presence
690 of core genes in satellites and phages shows that the latter form clusters well separated from
691 those of satellites (**Fig 5**). This confirms that our method discriminates the two types of
692 elements, and that satellites are very distinct from phages.

693



694

695 **Fig. 5. Pattern of presence/absence of the different satellite markers across all phage and putative phage-**

696 **satellite genomes.** Hierarchical clustering of each phage or phage-satellite genome (row) assessed for the presence of a

697 given phage satellite marker (column, at least one homolog gene with an e-value of at most $1e^{-2}$ and minimum coverage of

698 40%). For each genome, if a homolog for a marker is present, the cell is shown as blue, otherwise its absence is shown as an

699 empty cell. The markers used by SatelliteFinder to detect each phage satellite family are shown below the matrix as circles.

700 The columns on the right of the matrix indicate (from right to left): the family of the phage-satellite genome corresponding to

701 each row; and the Type of each satellite genome (limited to Types A, B and C).

702

703

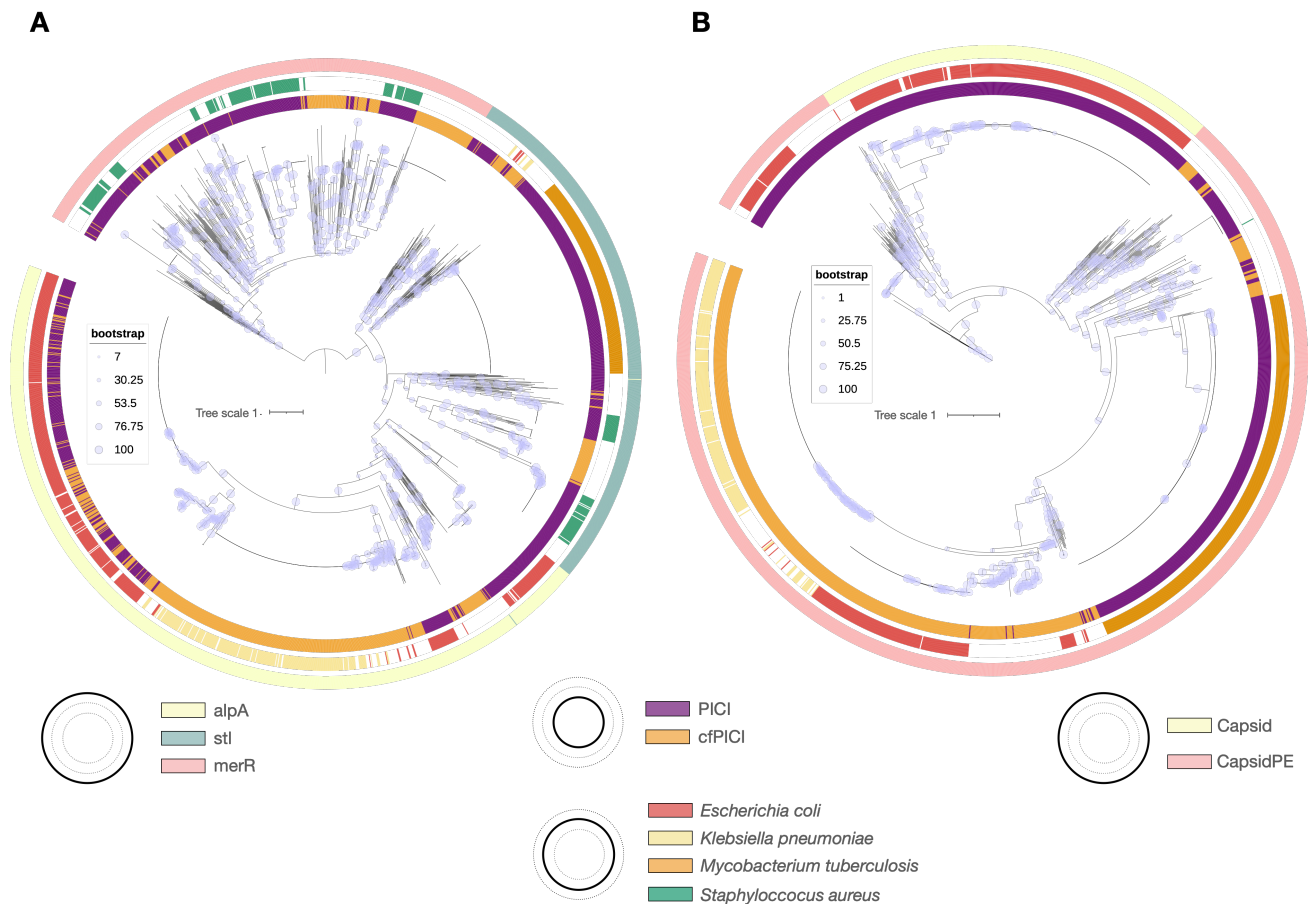
704 We assessed the evolutionary relationships between PIC1 and cfPIC1. In this particular case,

705 the two families of satellites share several core components. We tested if SatelliteFinder is

706 able to accurately distinguish them. First, no elements were simultaneously identified by the

707 cfPIC1 and PIC1 models. Second, no PIC1 satellites were identified when searching for them

708 directly in the dataset of cfPICI genomes. Finally, no cfPICI was identified when searching for
709 them directly in the PICI genomes. This suggests we can discriminate them accurately. To
710 confirm this, we quantified the genome-wide similarities between PICI and cfPICI, by
711 computing the wGRR between them. The clustering of the wGRR values revealed little to no
712 mixing between the major clusters of these two types of satellites (**Fig S9**). We then built
713 phylogenetic trees for four homologous core components: the transcriptional regulator, the
714 primase-replicase gene, the capsid gene (or capsid-modification gene in PICI) and the small
715 terminase. This revealed contrasting results. On one hand, the trees of the transcriptional
716 regulators and of the primase-replicase are strongly paraphyletic (**Fig 6A and Fig S10**),
717 suggesting gene flow between the two families of satellites (or intermingled evolutionary
718 history). On the other hand, the capsid (**Fig 6B**) and small terminase genes (**Fig S11**) separate
719 almost perfectly PICI from cfPICI. This suggests that some functions are more likely to be
720 exchanged between different types of satellites. Alternatively, the integrase-proximal genes
721 may constitute a functional module that might be involved in the cross-regulation of (potentially
722 similar) helper phages. These results confirm that the first half of the PICI and cfPICI satellites
723 are often similar and suggest a common evolutionary history. Hence, these are two
724 evolutionary related, but different, families of satellites whose part of the hijacking modules
725 (those that *de facto* distinguish PICI from cfPICI) have evolved independently for a long time.
726
727



728
729
730
731
732
733
734
735
736

Fig. 6. Phylogenetic trees of two of the prototypical components of PICI and cfPICI. A) Tree of the regulators of cfPICI and PICI. **B)** Tree of the capsid, or capsid-like components of cfPICI and PICI. In both A and B, outer circles indicate (from inside out) the family of satellites (PICI in purple, cfPICI in orange); the most frequent bacterial host species of the phage-satellites (less frequent host species are shown as white spaces); and the profile associated with the specific component (AlpA, MerR or Stl for the regulator in A; in B, the two profiles used to detect capsid-associated components (capsid or capsidPE, see Fig S1)).

737 Finally, since the families of satellites can be separated accurately, we assessed if multiple
738 phage satellites, each belonging to a different family, could co-integrate the same bacterial
739 genome, or if they mostly exclude each other. PLE never co-occur with other satellites, which
740 is justified by its narrow bacterial host range. However, we found that a few hundred bacterial
741 genomes have at least one P4-like and one PICI (227 genomes) or a P4-like and a cfPICI
742 (379 genomes). The former combination is mostly found in *E. coli* or *Shigella boydii* genomes,
743 while P4-like and cfPICI satellites tend to co-integrate a more diverse set of hosts, from *E. coli*
744 to *K. pneumoniae*, *Citrobacter freundii* or *Yersinia enterocolitica*. Combinations of PICI and
745 cfPICI are less common, and we found them in only 47 bacterial genomes. Impressively, 31
746 *E. coli* genomes have at least one element of each of the three families of satellites (P4-like,
747 PICI and cfPICI). These results show that satellites of different families often co-exist within
748 single bacterial genomes.

749

750 Discussion

751

752 In spite of the impact of satellites in phage reproduction and in the transfer of adaptive traits
753 among bacteria, there was little information in the literature on their composition and number.
754 We were able to leverage previous curated analyses of a few dozens of such elements to build
755 a tool – SatelliteFinder – that systematically and reproducibly identifies phage satellites in
756 bacterial genomes. This approach revealed numerous novel satellites, highlighting their
757 relevance in nature. Nevertheless, it has some limitations. First, the existence of few examples
758 of experimentally validated satellites means that it is not possible to accurately evaluate our
759 classification. We overcame this by using an iterative cycle of enrichment and curation of
760 satellite markers, but this also means that the phage-satellite models we propose must be
761 regarded as a first educated attempt to characterize each family. Interested users can easily
762 modify MacSyFinder models by changing one single text file. This will facilitate the search for
763 novel variants of known satellites and to add novel types of satellites. Second, the presence
764 of mobile genetic elements in the close vicinity of phage satellites can affect the identification
765 of the latter. For instance, multiple contiguous phage-satellites could be identified as an overly
766 large single satellite and a neighboring phage may lead to the exclusion of a valid satellite
767 because of more than a single nearby phage-like marker. The post-processing analysis we
768 perform using the output of MacSyFinder is important in diminishing these issues, but does
769 not always solve it. For instance, while this manuscript was being submitted, a preprint showed
770 that satellites can integrate inside prophages (45), which poses an even more difficult scenario
771 to accurately distinguish these elements from prophages. Future work will be needed to
772 assess the ability of our approach to correctly assign such cases. Third, we assume that
773 satellites are delimited between the two furthest (identified) components. This may result in
774 an underestimation of the size of the satellite, as well as their genomic repertoires. For
775 instance, some accessory genes in PIC1, namely genes involved in anti-phage defense, are
776 found between the attachment site and the integrase (10). Fourth, we cannot ascertain if all
777 satellites are functional. One would expect that most elements with the full set of core genes
778 are functional. This is less established for variants missing core genes. Yet, some of these
779 variants are highly conserved and a few were experimentally validated, suggesting that many
780 of them might be functional. Fifth, our approach is sensitive to the mis-annotation of small
781 genes as pseudogenes. For instance, in our previous analysis, we inferred that a large number
782 of Type B P4-like satellites were *alpA*-less, as most of them had an inactivated
783 (pseudogenized) *alpA* gene. However, this variant is very rare in the current analysis, because

784 the most recent bacterial database annotates *alpA* correctly. Finally, the PLE analysis was
785 done with draft genomes. The identification of phage satellites from draft genomes, where
786 they might be split across different contigs, or within misassembled contigs, can erroneously
787 suggest that some elements are either missing or have alternative core components. This
788 seems to be the case for the less complete PLE variants (Types H and I) that had homology
789 to either the first or the last “half” of the PLE model. This is not an issue when using complete
790 genomes, as was the case for the analysis of P4-like, PIC1 and cfPIC1.

791

792 Both the commonalities and uniqueness of the different families of phage satellites provide
793 insights on their function and evolution. Integrases are core genes of all satellites and almost
794 all elements were integrated in the chromosome. Regulatory components are also present in
795 almost all satellites, and they are much more satellite-specific than integrases. It has been
796 suggested that AlpA (or its functional analogues) mediate the cross-regulation between
797 satellites and helper phages (12, 16). The potential gene flow suggested by the mixed
798 phylogenies indicates that there might be functional compatibility, both within and across
799 satellite families (i.e. one regulator can be exchanged by another). It also raises the possibility
800 that different satellites could exploit the same phages, independently of the satellites’ hijacking
801 strategy. Hence, regulators might be one of the best candidates to understand the evolution
802 of satellites as a large family of elements. Another candidate could be the primase-replicase
803 component(s), which are present in all of the families studied here, but the divergence between
804 them suggests that they are analogs instead of homologs. Other components seem to be more
805 specific to each family of phage satellites. The *Psu-Delta-Sid* operon of P4-like phage satellites
806 performs a unique and conserved helper subversion strategy; the capsid assembly and head-
807 tail adaptor genes of cfPIC1 means that this is the only satellite known so far that hijacks only
808 part of the helpers’ virions; and PLEs have evolved genetic machinery to not only subvert a
809 specific incoming virulent phage, but also to kill its bacterial host upon excision. Interestingly,
810 this strategy might also be used by some PIC1, that were recently described to encode an
811 abortive infection system (10), and P4-like satellites can also encode (less drastic) anti-phage
812 defense systems (e.g. retrons) (9). Hence, while the overall strategies (of subversion,
813 replication or anti-phage defenses) of the different families of satellites might seem similar,
814 they occur through different genes and mechanisms, and are likely to have evolved multiple
815 times.

816

817 Novel, and experimentally testable insights into the different core functions of phage satellites
818 can also come from the presence/absence and organization of their core components. The
819 conserved genetic organization of most satellites, including its variants, suggests the
820 existence of tight relationships between contiguous core components and conserved

821 programs of gene expression. Certain variants lack core components and form specific clades,
822 thus suggesting they might be functional. The latter would be an indication that these
823 components are facultative. For instance, PICI of Type A represent a sub-family that relies on
824 capsid modifications to hijack their helpers, while those of Type B do not require such a
825 function. Psu-less variants of P4-like satellites are also frequent and form sub-families. One
826 of these is associated with a specific bacterial clade (*Serratia*), suggesting that its function is
827 either unnecessary or complemented by other components (e.g., Sid), and might have evolved
828 within the bacterial species and in the context of its prophages. Other variants are rare and
829 integrated into existing subfamilies of more complete types. These cases could represent
830 recent loss of core components, that result in defective variants and hence truly essential
831 components of these satellites.

832
833 The different families of satellites are strikingly different in their abundance, taxonomic
834 distribution, genetic composition, and genetic diversity. All of these might be suggestive of the
835 ecological conditions that underlie the establishment of the tripartite relationships between
836 bacteria, phages and their satellites. For instance, the reduced diversity and narrow bacterial
837 taxonomical range of PLEs might result from the high conservation of ICP1 making it unlikely
838 to infect (and thus transfer PLE to) other bacterial species (46). However, since PLEs were
839 not described to exploit other phages, virulent or lysogenic, this also suggests that the
840 tremendous selective pressure of ICP1 on *V. cholerae* might have created the conditions for
841 the tight and highly specialized function of PLEs in the ecology and evolution of this bacterial
842 pathogen. Other satellite families show a much higher genetic diversity. P4-like satellites are
843 found across many Enterobacteria, and PICI and cfPICI are particularly diverse and they have
844 the hosts with broadest taxonomic span. It remains to be uncovered whether this results from
845 a promiscuous relationship between these satellites and their broad host-ranged helper
846 phages (as our data suggests it is the case for some P4-like satellites), or from the
847 diversification of ancient versions of these satellites that diversified within each bacterial clade.
848 Our results also show that many bacterial genomes have multiple satellites of the same family.
849 This creates an interesting context for interactions between these elements. One recently
850 described example of satellite-satellite interactions involves a specific PICI (SaPI3) that is
851 induced not by prophages, but instead by other co-integrated PICI (47). Furthermore,
852 individual bacterial genomes often carry satellites of different families, suggesting that
853 competitive or antagonistic interactions between phage satellites of different families may
854 occur. Together with the ubiquity of prophages, and the oft-present anti-phage defense
855 systems in phage satellites (6, 9, 10), this highlights the complex networks that dictate the
856 emergence and maintenance of these phage satellites and phages, as well as the fitness and
857 survival of their bacterial hosts.

858

859 Our results reinforce the idea that phage satellites play an important role in the microbial world.
860 Even if our approach was conservative, requiring the presence of many core genes in common
861 to known satellites, we detected ca 5000 phage-satellites in bacterial genomes. This number
862 is huge, given the little we know about the distribution and diversity of these elements. There
863 are even more elements that we excluded because they lacked too many core genes relative
864 to the known satellites (e.g., we found more than 6000 Type C PICI elements). These
865 elements contain several hallmarks of phage-satellites, e.g. AlpA or packaging proteins, which
866 suggests there may be many other, still undescribed, families of satellite in bacterial genomes.
867 Such elements may use novel exciting mechanisms for replication, sensing, or phage
868 hijacking. Many elements in marine bacteria have recently been proposed to be phage
869 satellites (17), and other some “incomplete” PLEs were recently described in Vibrionacea
870 other than *V. cholerae* (42). Considering that half of the bacteria have at least one prophage
871 (48) and that we identified satellites in a much smaller number of bacterial genomes, it is very
872 likely that this is the beginning of the characterization of a vast diversity of phage satellites.
873 SatelliteFinder allows to easily add or modify models for satellites. It allows to experiment
874 combinations of both known and hypothetical marker genes, which will be key to identify novel
875 putative satellites for experimental verification.

876 Acknowledgements

877 We thank Kim Seed for comments and suggestions on earlier versions of the manuscript,
878 Graham Hatfull for helpful discussion regarding the PhiRv1 and PhiRv2 elements in *M.*
879 *tuberculosis*, and Bertrand Néron and Fabien Mareuil from the Institut Pasteur's Bioinformatics
880 and Biostatistics Hub for help in the development of the Docker and Galaxy version of
881 SatelliteFinder. We acknowledge funding from Equipe FRM (Fondation pour la Recherche
882 Médicale): EQU201903007835, Laboratoire d'Excellence IBEID Integrative Biology of
883 Emerging Infectious Diseases [ANR LBX-62 IBEID AAP BOURSE S2I ROCHA]. This work
884 used the computational and storage services (TARS cluster) provided by the IT department at
885 Institut Pasteur, Paris.
886

887 Data availability

888 The bacterial and phage genomes, as well as most profiles used to detect the core
889 components of phage satellites, are publicly available. For the core components without public
890 HMM profiles, we include the custom profiles as Files S2 to S19. The models used for
891 MacSyFinder are also available MacSyModels in the public repository. The additional custom
892 Python scripts to post-process the output of MacSyFinder are included in the Docker image at
893 (https://hub.docker.com/r/gempasteur/satellite_finder).

894 References

895

- 896 1. Fernández,L., Rodríguez,A. and García,P. (2018) Phage or foe: an insight into the impact of viral
897 predation on microbial communities. *ISME J.*, **12**, 1171–1179.
- 898 2. Touchon,M., Moura de Sousa,J.A. and Rocha,E.P. (2017) Embracing the enemy: the diversification
899 of microbial gene repertoires by phage-mediated horizontal gene transfer. *Curr. Opin.*
900 *Microbiol.*, **38**, 66–73.
- 901 3. Novick,R.P., Christie,G.E. and Penadés,J.R. (2010) The phage-related chromosomal islands of
902 Gram-positive bacteria. *Nat. Rev. Microbiol.*, **8**, 541–551.
- 903 4. Penadés,J.R. and Christie,G.E. (2015) The Phage-Inducible Chromosomal Islands: A Family of
904 Highly Evolved Molecular Parasites. *Annu. Rev. Virol.*, **2**, 181–201.
- 905 5. Moura de Sousa,J.A. and Rocha,E.P.C. (2022) To catch a hijacker: abundance, evolution and
906 genetic diversity of P4-like bacteriophage satellites. *Philos. Trans. R. Soc. B Biol. Sci.*, **377**,
907 20200475.
- 908 6. O’Hara,B.J., Barth,Z.K., McKitterick,A.C. and Seed,K.D. (2017) A highly specific phage defense
909 system is a conserved feature of the *Vibrio cholerae* mobilome. *PLOS Genet.*, **13**, e1006838.
- 910 7. Fillol-Salom,A., Bacarizo,J., Alqasmi,M., Ciges-Tomas,J.R., Martínez-Rubio,R., Roszak,A.W.,
911 Cogdell,R.J., Chen,J., Marina,A. and Penadés,J.R. (2019) Hijacking the Hijackers:
912 *Escherichia coli* Pathogenicity Islands Redirect Helper Phage Packaging for Their Own
913 Benefit. *Mol. Cell*, **75**, 1020-1030.e4.
- 914 8. Alqurainy,N., Miguel-Romero,L., Moura de Sousa,J., Chen,J., Rocha,E.P.C., Fillol-Salom,A. and
915 Penades,J.R. (2022) A widespread family of phage-inducible chromosomal islands only steals
916 bacteriophage tails to spread in nature. 10.1101/2022.09.08.507074.
- 917 9. Rousset,F., Depardieu,F., Miele,S., Dowding,J., Laval,A.-L., Lieberman,E., Garry,D., Rocha,E.P.C.,
918 Bernheim,A. and Bikard,D. (2022) Phages and their satellites encode hotspots of antiviral
919 systems. *Cell Host Microbe*, **30**, 740-753.e5.
- 920 10. Fillol-Salom,A., Rostøl,J.T., Ojiogu,A.D., Chen,J., Douce,G., Humphrey,S. and Penadés,J.R.
921 (2022) Bacteriophages benefit from mobilizing pathogenicity islands encoding immune
922 systems against competitors. *Cell*, **185**, 3248-3262.e20.
- 923 11. Christie,G.E. and Calendar,R.L. (2001) P4-like satellite viruses. In Tidona,C.A., Darai,G., Büchen-
924 Osmond,C. (eds), *The Springer Index of Viruses*. Springer Berlin Heidelberg, Berlin,
925 Heidelberg, pp. 1288–1292.

- 926 12. Fillol-Salom,A., Martínez-Rubio,R., Abdulrahman,R.F., Chen,J., Davies,R. and Penadés,J.R.
927 (2018) Phage-inducible chromosomal islands are ubiquitous within the bacterial universe.
928 *ISME J.*, **12**, 2114–2128.
- 929 13. Briani,F., Dehò,G., Forti,F. and Ghisotti,D. (2001) The Plasmid Status of Satellite Bacteriophage
930 P4. *Plasmid*, **45**, 1–17.
- 931 14. Canchaya,C., Desiere,F., McShan,W.M., Ferretti,J.J., Parkhill,J. and Brüssow,H. (2002) Genome
932 Analysis of an Inducible Prophage and Prophage Remnants Integrated in the *Streptococcus*
933 *pyogenes* Strain SF370. *Virology*, **302**, 245–258.
- 934 15. Haudiquet,M., de Sousa,J.M., Touchon,M. and Rocha,E.P.C. (2022) Selfish, promiscuous and
935 sometimes useful: how mobile genetic elements drive horizontal gene transfer in microbial
936 populations. *Philos. Trans. R. Soc. B Biol. Sci.*, **377**, 20210234.
- 937 16. Ibarra-Chávez,R., Hansen,M.F., Pinilla-Redondo,R., Seed,K.D. and Trivedi,U. (2021) Phage
938 satellites and their emerging applications in biotechnology. *FEMS Microbiol. Rev.*,
939 10.1093/femsre/fuab031.
- 940 17. Eppley,J.M., Biller,S.J., Luo,E., Burger,A. and DeLong,E.F. (2022) Marine viral particles reveal an
941 expansive repertoire of phage-parasitizing mobile elements. 10.1101/2022.07.26.501625.
- 942 18. Hackl,T., Laurenceau,R., Ankenbrand,M.J., Bliem,C., Cariani,Z., Thomas,E., Dooley,K.D.,
943 Arellano,A.A., Hogle,S.L., Berube,P., *et al.* (2020) Novel integrative elements and genomic
944 plasticity in ocean ecosystems. 10.1101/2020.12.28.424599.
- 945 19. Angermeyer,A., Hays,S.G., Nguyen,M.H.T., Johura,F., Sultana,M., Alam,M. and Seed,K.D. (2022)
946 Evolutionary Sweeps of Subviral Parasites and Their Phage Host Bring Unique Parasite
947 Variants and Disappearance of a Phage CRISPR-Cas System. *mBio*, **13**, e03088-21.
- 948 20. Perrin,A. and Rocha,E.P.C. (2021) PanACoTA: a modular tool for massive microbial comparative
949 genomics. *NAR Genomics Bioinforma.*, **3**.
- 950 21. Ondov,B.D., Treangen,T.J., Melsted,P., Mallonee,A.B., Bergman,N.H., Koren,S. and
951 Phillippy,A.M. (2016) Mash: fast genome and metagenome distance estimation using
952 MinHash. *Genome Biol.*, **17**, 132.
- 953 22. Abby,S.S., Néron,B., Ménager,H., Touchon,M. and Rocha,E.P.C. (2014) MacSyFinder: A
954 Program to Mine Genomes for Molecular Systems with an Application to CRISPR-Cas
955 Systems. *PLoS ONE*, **9**, e110726.
- 956 23. Néron,B., Denise,R., Coluzzi,C., Touchon,M., Rocha,E.P.C. and Abby,S.S. (2022) MacSyFinder
957 v2: Improved modelling and search engine to identify molecular systems in genomes.
958 10.1101/2022.09.02.506364.

- 959 24. Steinegger,M. and Söding,J. (2017) MMseqs2 enables sensitive protein sequence searching for
960 the analysis of massive data sets. *Nat. Biotechnol.*, **35**, 1026–1028.
- 961 25. Huerta-Cepas,J., Szklarczyk,D., Heller,D., Hernández-Plaza,A., Forslund,S.K., Cook,H.,
962 Mende,D.R., Letunic,I., Rattei,T., Jensen,L.J., *et al.* (2019) eggNOG 5.0: a hierarchical,
963 functionally and phylogenetically annotated orthology resource based on 5090 organisms and
964 2502 viruses. *Nucleic Acids Res.*, **47**, D309–D314.
- 965 26. Sievers,F., Wilm,A., Dineen,D., Gibson,T.J., Karplus,K., Li,W., Lopez,R., McWilliam,H.,
966 Remmert,M., Söding,J., *et al.* (2011) Fast, scalable generation of high-quality protein multiple
967 sequence alignments using Clustal Omega. *Mol. Syst. Biol.*, **7**, 539.
- 968 27. Eddy,S.R. (2011) Accelerated Profile HMM Searches. *PLoS Comput. Biol.*, **7**, e1002195.
- 969 28. Moura de Sousa,J.A., Pfeifer,E., Touchon,M. and Rocha,E.P.C. (2021) Causes and
970 Consequences of Bacteriophage Diversification via Genetic Exchanges across Lifestyles and
971 Bacterial Taxa. *Mol. Biol. Evol.*, **38**, 2497–2512.
- 972 29. Sherwin,W.B., Chao,A., Jost,L. and Smouse,P.E. (2017) Information Theory Broadens the
973 Spectrum of Molecular Ecology and Evolution. *Trends Ecol. Evol.*, **32**, 948–963.
- 974 30. Katoh,K. and Standley,D.M. (2013) MAFFT Multiple Sequence Alignment Software Version 7:
975 Improvements in Performance and Usability. *Mol. Biol. Evol.*, **30**, 772–780.
- 976 31. Steenwyk,J.L., Buida,T.J., Li,Y., Shen,X.-X. and Rokas,A. (2020) ClipKIT: A multiple sequence
977 alignment trimming software for accurate phylogenomic inference. *PLOS Biol.*, **18**, e3001007.
- 978 32. Nguyen,L.-T., Schmidt,H.A., von Haeseler,A. and Minh,B.Q. (2015) IQ-TREE: A Fast and
979 Effective Stochastic Algorithm for Estimating Maximum-Likelihood Phylogenies. *Mol. Biol.*
980 *Evol.*, **32**, 268–274.
- 981 33. Letunic,I. and Bork,P. (2021) Interactive Tree Of Life (iTOL) v5: an online tool for phylogenetic
982 tree display and annotation. *Nucleic Acids Res.*, **49**, W293–W296.
- 983 34. Afgan,E., Baker,D., Batut,B., van den Beek,M., Bouvier,D., Čech,M., Chilton,J., Clements,D.,
984 Coraor,N., Grüning,B.A., *et al.* (2018) The Galaxy platform for accessible, reproducible and
985 collaborative biomedical analyses: 2018 update. *Nucleic Acids Res.*, **46**, W537–W544.
- 986 35. Halling,C. and Calendar,R. (1990) Bacteriophage P2 ogr and P4 delta genes act independently
987 and are essential for P4 multiplication. *J. Bacteriol.*, **172**, 3549–3558.
- 988 36. Lindqvist,B.H., Dehò,G. and Calendar,R. (1993) Mechanisms of genome propagation and helper
989 exploitation by satellite phage P4. *Microbiol. Rev.*, **57**, 683–702.

- 990 37. Kizziah, J.L., Rodenburg, C.M. and Dokland, T. (2020) Structure of the Capsid Size-Determining
991 Scaffold of “Satellite” Bacteriophage P4. *Viruses*, **12**, 953.
- 992 38. Novick, R.P. and Ram, G. (2017) Staphylococcal pathogenicity islands — movers and shakers in
993 the genomic firmament. *Curr. Opin. Microbiol.*, **38**, 197–204.
- 994 39. Hendrix, R.W., Smith, M.C.M., Burns, R.N., Ford, M.E. and Hatfull, G.F. (1999) Evolutionary
995 relationships among diverse bacteriophages and prophages: All the world’s a phage. *Proc.*
996 *Natl. Acad. Sci.*, **96**, 2192–2197.
- 997 40. Bibb, L.A. and Hatfull, G.F. (2002) Integration and excision of the Mycobacterium tuberculosis
998 prophage-like element, ϕ Rv1: Integration and excision of ϕ Rv1. *Mol. Microbiol.*, **45**, 1515–
999 1526.
- 1000 41. Kala, S., Cumby, N., Sadowski, P.D., Hyder, B.Z., Kanelis, V., Davidson, A.R. and Maxwell, K.L.
1001 (2014) HNH proteins are a widespread component of phage DNA packaging machines. *Proc.*
1002 *Natl. Acad. Sci.*, **111**, 6022–6027.
- 1003 42. LeGault, K.N., Barth, Z.K., DePaola, P. and Seed, K.D. (2022) A phage parasite deploys a nicking
1004 nuclease effector to inhibit viral host replication. *Nucleic Acids Res.*, 10.1093/nar/gkac002.
- 1005 43. McKitterick, A.C., Hays, S.G., Johura, F.-T., Alam, M. and Seed, K.D. (2019) Viral Satellites Exploit
1006 Phage Proteins to Escape Degradation of the Bacterial Host Chromosome. *Cell Host*
1007 *Microbe*, **26**, 504-514.e4.
- 1008 44. de Laat, W.L., Jaspers, N.G.J. and Hoeijmakers, J.H.J. (1999) Molecular mechanism of nucleotide
1009 excision repair. *Genes Dev.*, **13**, 768–785.
- 1010 45. Tommasini, D., Mageeney, C.M. and Williams, K.P. (2022) An integrase clade that repeatedly
1011 targets prophage late genes, yielding helper-embedded satellites.
1012 10.1101/2022.07.18.500453.
- 1013 46. Boyd, C.M., Angermeyer, A., Hays, S.G., Barth, Z.K., Patel, K.M. and Seed, K.D. (2021)
1014 Bacteriophage ICP1: A Persistent Predator of *Vibrio cholerae*. *Annu. Rev. Virol.*, **8**, 285–304.
- 1015 47. Haag, A.F., Podkowik, M., Ibarra-Chávez, R., Gallego del Sol, F., Ram, G., Chen, J., Marina, A.,
1016 Novick, R.P. and Penadés, J.R. (2021) A regulatory cascade controls *Staphylococcus aureus*
1017 pathogenicity island activation. *Nat. Microbiol.*, **6**, 1300–1308.
- 1018 48. Touchon, M., Bernheim, A. and Rocha, E.P. (2016) Genetic and life-history traits associated with
1019 the distribution of prophages in bacteria. *ISME J.*, **10**, 2744–2754.
- 1020

1021